16×16 개량핵연료 연료봉의 수력적 안정성에 관한 연구

A Study on the Hydraulic Stability of Fuel Rod for the Advanced 16×16 Fuel Assembly Design

전 상 윤†
Jeon, Sang-Youn
(논문접수일 : 2004년 8월 29일 ; 심사종료일 : 2005년 8월 29일)

요 지

경수로 원자로 하부구조물에서 발생되는 유로의 불균일성에 기인하는 교차류와 핵연료집합체의 수력저항의 차이에 의해 발생하는 교차류, 그리고 축류 등에 의해 유발되는 연료봉의 불안정성은 핵연료손상의 원인이 될 수 있으므로, 새로운 연료 개발 시 연료봉에 대한 진동 및 안정성 해석을 수행하여 연료봉 진동과 불안정성 발생 여부를 확인하고 있다. 본 연구에서는 새로 개발된 고리 2호기용 16×16형 개량핵연료 집합체에 대한 연료봉의 진동 및 안정성 해석을 수행하여 지지격자 높이와 위치, 그리고 지지조건 등이 연료봉의 진동특성 및 안정성에 미치는 영향을 평가하였다. 그리고 해석결과에 근거하여 개량연료 집합체에서 중간지지격자 높이와 각 지지격자의 위치를 제안하였다.

핵심용어 : 16×16형 개량핵연료, 연료봉 안정성, 축류, 횡류, 가압경수로, 연료손상

Abstract

The fuel rod instability can be occurred because of the axial and cross flow due to the flow anomaly and/or flow redistribution in the lower core plate region of the pressurized water reactor. The fuel rod vibration due to the hydraulic instability is one of the root causes of fuel failure. The verification on the fuel rod vibration and instability is needed for the new fuel assembly design to verify the fuel rod instability. In this study, the fuel rod vibration and stability analyses were performed to investigate the effect of the grid height, fuel rod support condition, and span adjustment on the fuel rod vibration characteristics for the advanced 16×16 fuel assembly design. Based on the analysis results, the grid height and grid axial elevation of the advanced 16×16 fuel assembly design were proposed.

keywords : *advanced 16×16 fuel assembly design, fuel rod instability, axial flow, cross flow, pressurized water reactor, fuel failure*

1. Introduction

The fuel rod instability can be occurred because of the axial and cross flow due to the flow anomaly and/or flow redistribution in the lower core plate region of the pressurized water reactor. The flow anomaly causes a vortex to periodically form in the lower plenum area and results in a slight pressure depression in the core area above the vortex. A resulting cross flow is caused by coolant flowing into the low pressure core region caused by this vortex. Besides the lower plenum flow anomaly cross flow, a typical fuel assembly will also experience cross flow due to the flow redistribution from the coolant passing through the lower core plate holes. The fuel rod vibration due to the hydraulic instability is known as one of the root causes of fuel failure The instability ratio is the ratio of effective velocity to critical velocity (Ve-Effective/Vc-Critical). The vibrational amplitudes of the tube become large and

† 책임저자, 정회원 · 한전원자력연료㈜ 설계기술원 책임연구원
전화: 042-868-1182 ; Fax: 042-868-1149
E-mail: syjeon@knfc.co.kr

• 이 논문에 대한 토론을 2006년 3월 31일까지 본 학회에 보내주시면 2006년 6월호에 그 결과를 게재하겠습니다.

display orbital patterns when the ratio of effective velocity to critical velocity (Ve-Effective/Vc-Critical) is greater than 1.0(Au-Yang, 2001). The effective velocity depends on the span wise distribution of cross flow velocity, density and mode shape. The verification on the fuel rod vibration and instability is needed for the new fuel assembly design to avoid the fuel rod instability during the power operation in the nuclear power plant. Paidoussis(1973;1990) investigated the dynamics and stability of a flexible cylinder in a narrow coaxial cylinder duct subjected to annular flow and the dynamics of cylindrical structure subjected to axial flow(Paidoussis, 1973; Paidoussis 등, 1990). Woo(1994) developed a new numerical model based on spectral method for studying the dynamics and stability of flexible cylinder in a duct with inviscid annular flow(Woo 등, 1994). Park(2004) studied the dynamic characteristics of the beam structure with respect to several initial stresses for the beam structure with multiple supports(Park 등, 2004). Lee(2001) investigated the effects of multi-delaminations on the dynamic characteristics of multi-delamination beams(Lee 등, 2001). The general kinematic continuity conditions are derived from assumption of constant curvature at the multi-delamination tip. Kim(2002) derived the governing equation and force-displacement relations of a beam-column element on elastic foundation based on variational approach of total potential energy (Kim 등, 2002).

The fuel rod finite element models of the advanced 16×16 fuel assembly design were developed for fuel rod vibration and stability analysis. The model considers the geometric configuration, mass density distribution, and material properties corresponding to the operating temperature. The fuel rod and grid spring and dimple system are modeled using two dimensional beam and linear spring elements, respectively. The stiffness of linear spring is a linear combination of the radial and tangential stiffness of grid springs and dimples to simulate fuel rod support constraints within grid cell.

The fuel rod vibration and instability analysis has been performed with the fuel rod finite element model to investigate the effect of the grid height, support condition, and span adjustment of the advanced 16x16 fuel assembly design. The 1.79in. and 2.25 in. grid heights were used for the investigation of grid heights effect and full support condition and pinned support condition were used for the investigation of support condition effect. The full support condition and pinned support condition were used to demonstrate the contact and gapped conditions between fuel rod and mid grid dimples. The span adjustments are achieved by moving down the 2^{nd} grid (first mid grid) and by moving up the 1^{st} grid (bottom inconel grid) to optimize the maximum span length between grids. The instability ratio (Ve-Effective/Vc-Critical) and vibration amplitude of the advanced 16×16 fuel assembly design were calculated for each grid height, support condition, and span adjustment cases. Based on the analysis results, the grid height and grid axial elevation of the advanced 16×16 fuel assembly design were proposed by evaluating the vibration characteristic and instability ratio for each grid height and span adjustment cases. And, the effect of fuel rod support condition on the vibration characteristic and instability ratio of the fuel rod was investigated for full support condition and pinned support condition.

2. Fuel Rod Model and Modal Analysis

The analysis models are based on the advanced 16x16 fuel assembly design with 6 ZIRLO™ Mid Grids, Inconel Top and Bottom Grids, 3 ZIRLO™ IFM Grids, Protective Grid, and Long Solid End Plug. Fig. 1 and Fig. 2 shows the configuration of the advanced 16×16 fuel assembly and fuel rod design, respectively. Fig. 3 shows the configuration of the fuel rod support system. The fuel rod is supported by two dimples and one spring in each direction as shown in Fig. 3. The fuel rod consists of cladding tube, top and bottom end plug, plenum spring, and fuel pellets. The finite element model

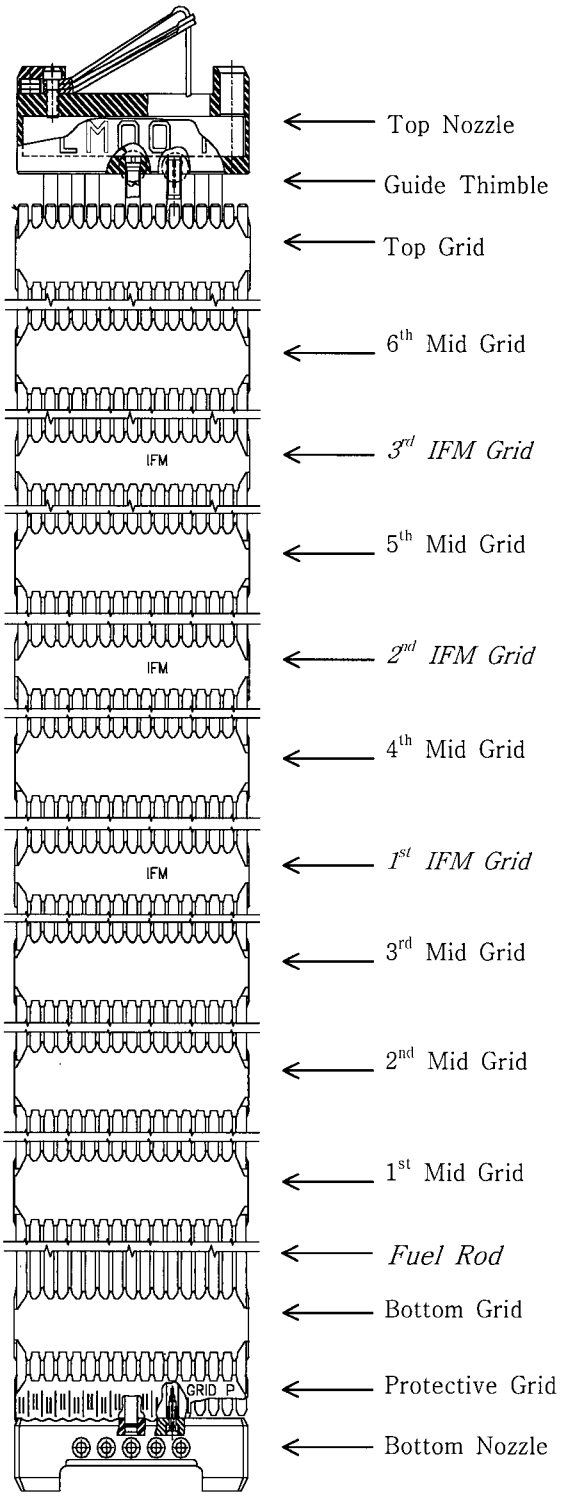

Fig. 1 Configuration of the 16×16 Fuel Assembly

for the 16×16 fuel rod design is shown in Fig. 4. As shown in the Fig. 4, the fuel rod finite element model consists of the two dimensional beam and one dimensional linear spring elements. The tangential spring stiffness for the two dimples and one spring are added to the radial spring stiffness for the two dimples and one spring in the finite element model, respectively. The real constants and material properties for finite element model are shown in Table 1 and the spring and dimple stiffness values are shown in Table 2.

Table 1 Real Constants and Material Properties for the Finite Element Model

Items	Values
Area (in.^{2})	0.024
Moment (in.^{4})	0.0003412
Thickness (in.)	0.360
Young's Modulus (at 600°F, psi)	11.0 x 10^6
Poisson Ratio	0.34

Table 2 Spring and Dimple Stiffness for the Finite Element Model

Items	Spring	Dimple
Top Grid (lbs/in.)	413.8	4023.3
IFM Grid (lbs/in.)	(No Spring)	1416.2
Mid Grid (lbs/in.)	248.14	2861.1
Bottom Grid (lbs/in.)	532.48	4054.0
Protective Grid (lbs/in.)	(No Spring)	357.61

The spring force relaxation (decrease) will be occurred due to the irradiation in the nuclear reactor. This spring force relaxation is modeled by reducing the tangential spring stiffness. To simulate the EOL (End-Of-Life) condition of the fuel, a reduced tangential stiffness of 10% of BOL (Beginning-Of-Life) value is assumed for the fuel rod at all grid dimple elevations. The model considers the geometric configuration, mass density distribution, and material properties corresponding to the operating temperature of 600°F. The thermal expansion of the fuel rod, spring, and dimples is not considered because the thermal expansion of those components is very small compare to the geometric configuration of each component. The input parameters are based on nominal design dimensions. The individual density for the finite element model is corrected to include the added mass effects for the submerged fuel rod. The displaced fuel rod volume and coolant density is used to calculate the added mass correction factor. The radial and tangential stiffness of the spring and

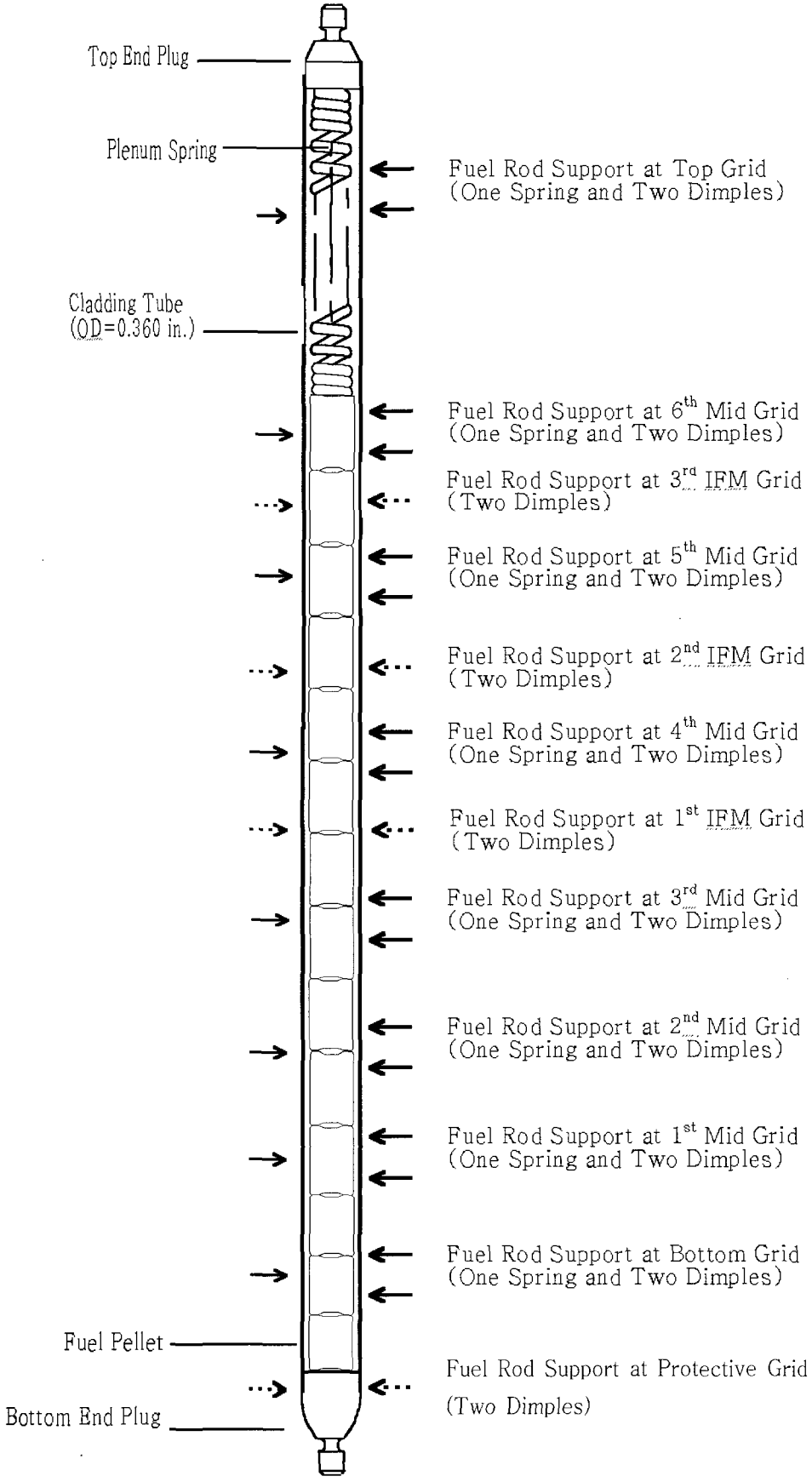

Fig. 2 Configuration of the 16×16 Fuel Rod

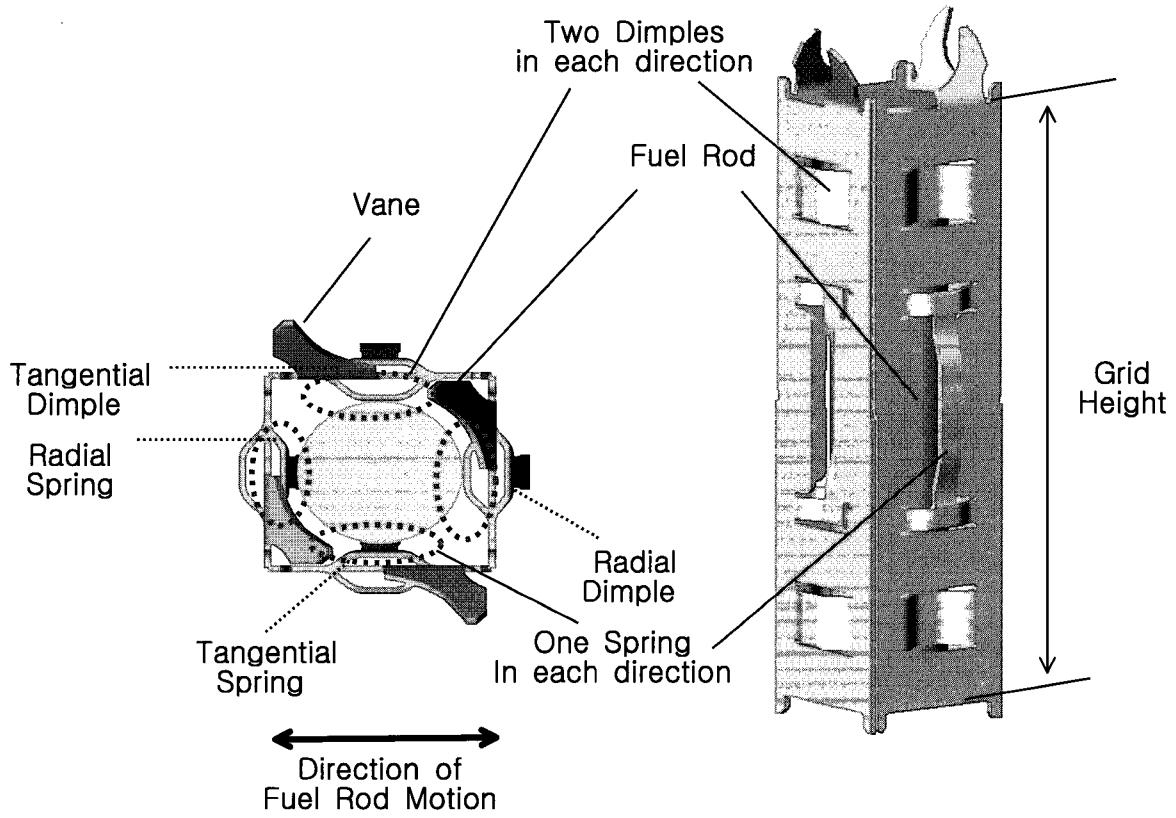

Fig. 3 Configuration of Fuel Rod Support System

dimple represents the fuel rod supports. The radial stiffness is adjusted to the operating temperature of 600°F. The tangential stiffness for the grid spring and dimple of top, bottom, mid, and protective grids are calculated based on the individual cell spring force, cell dimple force, and rod drag force. The radial and tangential stiffness are combined together and the combined stiffness values are used for the generation of the spring element in fuel rod finite element model. Two different models were generated considering different grid inner strap height of 1.79in. and 2.25in. to investigate the effects of grid height. The span adjustments are achieved by moving down the first mid grid and by moving up the bottom inconel grid. The full support condition and pinned support condition were used to simulate the un-irradiated condition and irradiated condition of grid spring and dimple by adjusting the dimple stiffness. The fuel rod is supported by spring and dimples with EOL spring force for the full support condition to simulate the EOL condition with spring force and the fuel rod is just in contact with spring at spring elevation for the pinned support condition to simulate the EOL condition without spring force. For the full support condition, a fuel rod with 10% of the BOL tangential stiffness with 3 contact points on each mid grid was used to simulate the fuel assembly under irradiation condition, and for the pinned support condition, a fuel rod that only contacts at the spring location of each mid grid was used to simulate the gap between fuel rod and spring due to the spring force relaxation at EOL condition.

The fuel rod vibration analysis was performed using the WECAN computer code(Westinghouse, 1989). The WECAN computer code is a general purpose finite element program. The simultaneous linear equation for the entire structure is solved by a variation of the Gaussian elimination method known as the wave-front technique. The reduced modal analysis is used to determine the natural frequencies and mode shapes for a linear and undamped

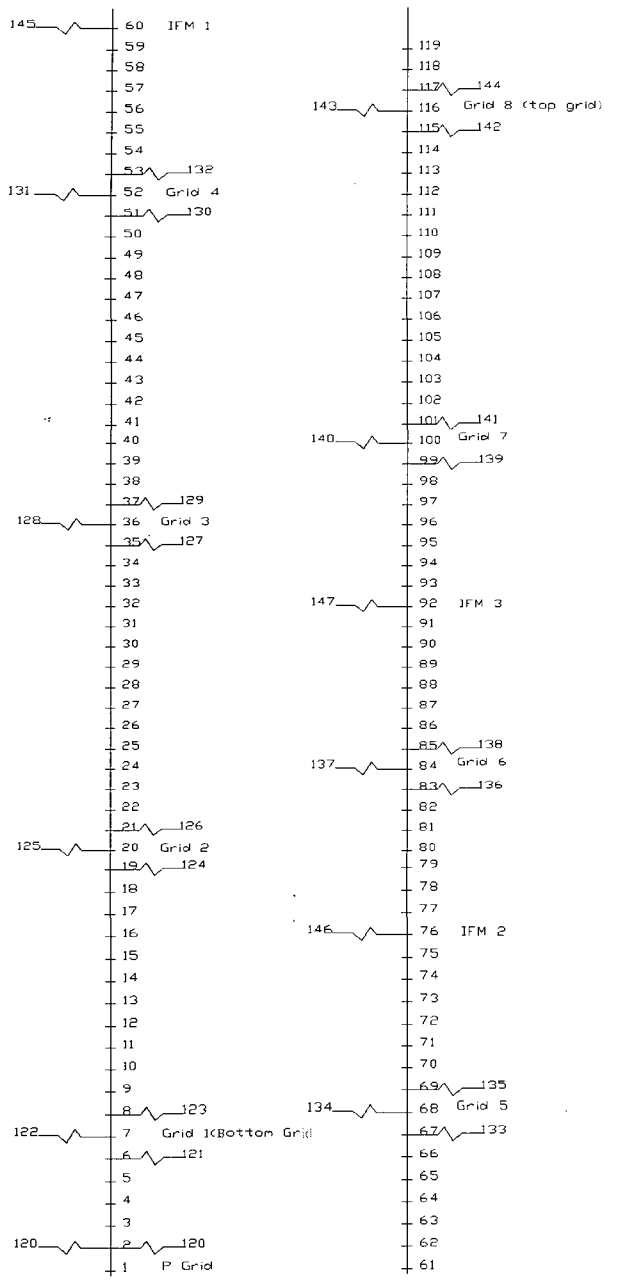

Fig. 4 Fuel Rod Finite Element Model

structure. This analysis requires the master degrees of freedom of the model. For the fuel rod model, the master degrees of freedom were specified at all nodes on the fuel rod. Table 3 shows the analysis matrix for the span adjustments cases.

3. Fuel Rod Stability Analysis

The fluid elastic excitation is self excited vibration mechanism. When a tube bundle is subject to cross flow with increasing velocity, it will come to a point at which the responses of the tube suddenly increase until tube to tube impacting or other nonlinear effects limit the tube motion. This mechanism is characterized by a critical flow velocity. The vibrational amplitudes of tube become large and display orbital patterns when the critical flow velocity is exceeded(Au-Yang, 2001). The large amplitude vibrations initiate when the critical velocity, Vc, is exceeded. The critical velocity of the fuel rod bundle can be predicted by the following equation:

$$V_c = \beta f_n D \sqrt{\frac{m_o \delta_n}{\rho D^2}} \tag{1}$$

where, V_c : critical velocity,

β : instability constant,

f_n : fuel rod natural frequency of the n-th mode, Hz,

D : fuel rod diameter, in.,

m_o : fuel rod mass per unit length,

δ_n : fuel rod damping of the n-th mode, $\delta_n = 2\pi\zeta_n$,

ζ_n : damping ratio of the n-th mode,

ρ : fluid density, lbs-sec^2/in.^{4}

Table 3 Span Length between 1st Grid and 2nd Grid

Items		1st Grid Move-Up (in.)	2nd Grid Move-Down (in.)	Span Length (in.)
Standard 16×16 (Before Span Adjustment)		-	-	24.43
Advanced 16×16 (After Span Adjustment)	CASE 1	0.50	0.70	23.23
	CASE 2	1.00	0.70	22.73
	CASE 3	0.50	0.35	23.58
	CASE 4	1.00	0.35	23.08

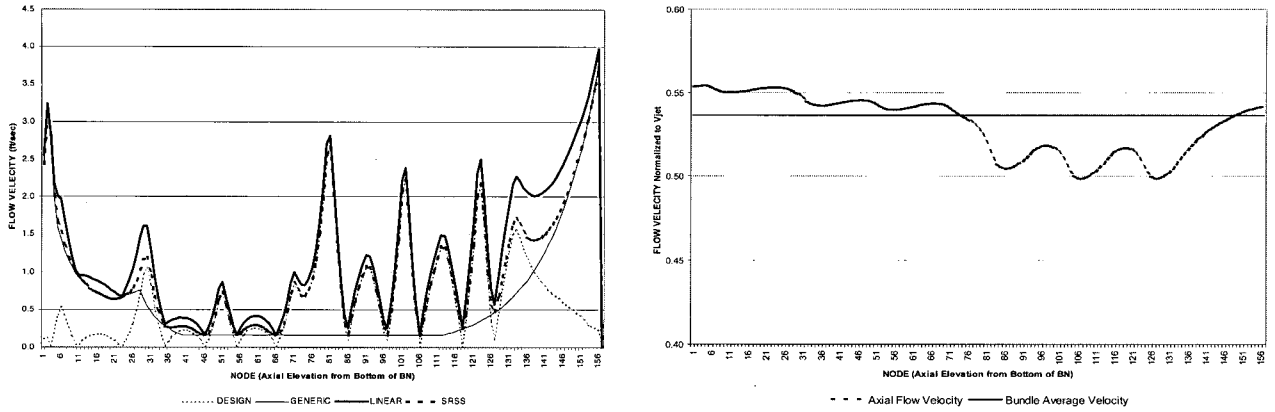

(a) Cross Flow Velocity Distribution (b) Axial Flow Velocity Distribution

Fig. 5 Cross Flow and Axial Flow Velocity Distribution

The effective velocity, Ve, depends on the distribution of cross flow velocity, density, and the mode shape. The effective velocity can be written as the following form:

$$V_e = \frac{\sum_{i=1}^{n} V_i^2 \phi_{in}^2 \Delta Z_i}{\sum_{i=1}^{n} \phi_{in}^2 \Delta Z_i} \quad (2)$$

where, V_i : flow velocity at i-th node,

ϕ_{in} : normalized displacement of the i-th node in the n-th mode,

ΔZ_i : i-th span location

The instability ratio is the ratio of effective velocity to critical velocity (V-Effective/V-Critical). When the instability ratio exceeds 1.0, instability is predicted to occur. The fuel rod shall be designed to maintain a stable configuration due to flow induced vibrations resulting from axial and cross flow velocity distributions as well as the induced cross flow due to the difference in loss coefficients between two different fuel assembly designs during a mixed core operation in the pressurized water reactor. The cross flow velocity profile is generated for the fuel rod instability analysis based on the difference in loss coefficients between advanced 16×16 fuel design and standard 16×16 fuel design. The axial and cross flow profiles inside the fuel assembly are calculated by solving the momentum equations in coolant flow area. THINC-IV computer code(Westinghouse, 2000) was used for the axial and cross flow calculations. The fuel assembly array which composed of two different types of assemblies is adopted as an analysis model, because it gives the highest cross flow for a loss coefficient mismatch. The current 16×16 fuel assembly and the advanced 16×16 fuel assembly was used for this study.

Fig. 5 shows the profile of generic cross flow, design cross flow, linearly combined cross flow, and square root sum of squares (SRSS) of the cross flow velocity for the design and generic cross flow with axial elevation from bottom of bottom nozzle to bottom of top nozzle. The combination of generic and design cross flow was used for this analysis. The normalized axial flow velocity distribution is also shown in Fig. 5. The fuel rod stability analysis was performed using the VIBAMP computer code (Westinghouse, 1989) to investigate the effects of the grid heights, support conditions, and span adjustment on the fuel rod stability. The VIBAMP code calculates the instability ratio based on the critical velocity and effective velocity, and provides an estimate of the fuel rod vibrational amplitude based on the cross flow and axial flow due to turbulent excitation and vortex shedding. The vibrational amplitude of the turbulent excitation was calculated by the semi-empirical equation which is derived based on the following correlation(ASME, 1995).

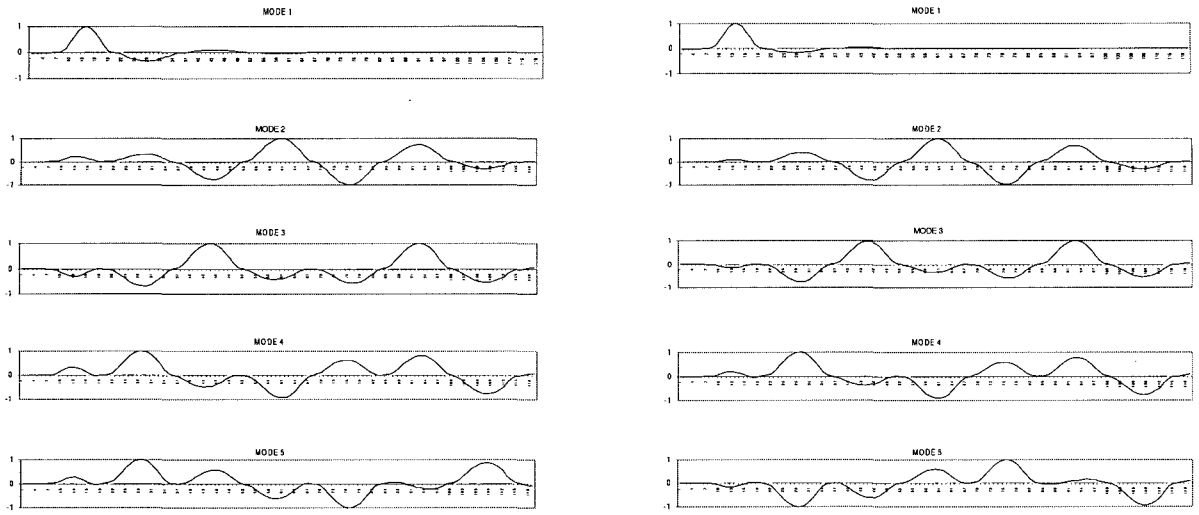

(a) Grid Height = 1.79 in. (b) Grid Height = 2.25 in.

Fig. 6 Mode Shapes of Fuel Rod (Grid Height)

The total amplitude of the turbulent excitation is obtained by taking the square root sum of quares (SRSS) of the amplitudes for axial and cross flow due to turbulent excitation.

$$y_n = f(D, L, \hat{m}, \delta_n, \hat{v}, \phi_n, C_1, C_2) \tag{3}$$

where, D : fuel rod diameter,
L : fuel rod length,
$\hat{m}$: dimensionless fuel rod mass,
δ_n : fuel rod damping of the n-th mode,
$\hat{v}$: dimensionless axial or cross flow velocity,
ϕ_n : normalized displacement of the n-th mode,
C_1 : empirical constant related to the excitation force,
C_2 : empirical constant related to the power spectral density

And, the vibrational amplitude of the vortex induced vibration is based on the following equation(ASME, 1995).

$$y_n = \frac{C_L J D \phi_n}{16\pi^2 S^2 [m_t \delta_n / (\rho D^2)]} \tag{4}$$

where, C_L : lift coefficient,
J : correlation factor,
D : fuel rod diameter, in.,
S : Strouhal number,
m_t : total fuel rod mass per unit length,
ρ : fluid density, lbs-sec^2/in.^{4}

The total amplitudes are obtained by taking the linear summation of amplitudes for the turbulent excitation and vortex induced vibration.

4. Results and Evaluation

4.1 Natural Frequencies and Mode Shapes

The 16×16 fuel rod natural frequencies and mode shapes of the 16×16 fuel rod are calculated for both the 1.79in. and 2.25 in. grid heights. The natural frequencies for both the 1.79in. and 2.25in. grid heights are tabulated in Table 4. The mode shapes for the 1.79in. and 2.25in. grid heights are shown in Fig. 6. The natural frequencies of 2.25in. grid height are a little bit higher than that of the 1.79in. grid height due to the longer fuel rod support length. The mode shapes of both the 1.79in. and 2.25in. grid heights are almost same. Based on the results, the dynamic characteristics of fuel rod for both the 1.79in. and 2.25 in. grid heights are very similar.

The natural frequencies for the span adjustments are tabulated in Table 5 and the mode shapes of

Table 4 Natural Frequencies of Fuel Rod-Grid Height (unit : Hz)

Mode	Grid Height* = 1.79 in.	Grid Height* = 2.25 in.
1	32.277	34.105
2	37.704	43.411
3	40.130	45.014
4	43.548	47.339
5	47.369	49.942
6	50.840	52.255
7	52.996	53.656
8	92.227	95.051
9	113.360	123.340
10	118.840	127.440

* Grid Height : the height of the grid inner strap as shown in Fig. 3 (The higher grid height has longer distance between two dimples to support the fuel rod.)

Table 5 Natural Frequencies of Fuel Rod-Span Adjustment (unit : Hz)

Mode	Before Span Adjustment	After Span Adjustment (refer to Table 3)			
		CASE 1	CASE 2	CASE 3	CASE 4
1	34.105	37.273	38.645	36.375	37.775
2	43.411	43.172	43.252	43.335	43.359
3	45.014	44.392	44.484	44.752	44.801
4	47.339	46.569	46.614	46.938	46.978
5	49.942	49.319	49.336	49.575	49.597
6	52.255	51.947	51.952	52.062	52.070
7	53.656	53.606	53.607	53.624	53.625
8	95.051	104.050	108.060	101.450	105.450
9	123.340	122.090	122.340	122.990	123.060
10	127.440	125.370	125.510	126.480	126.600

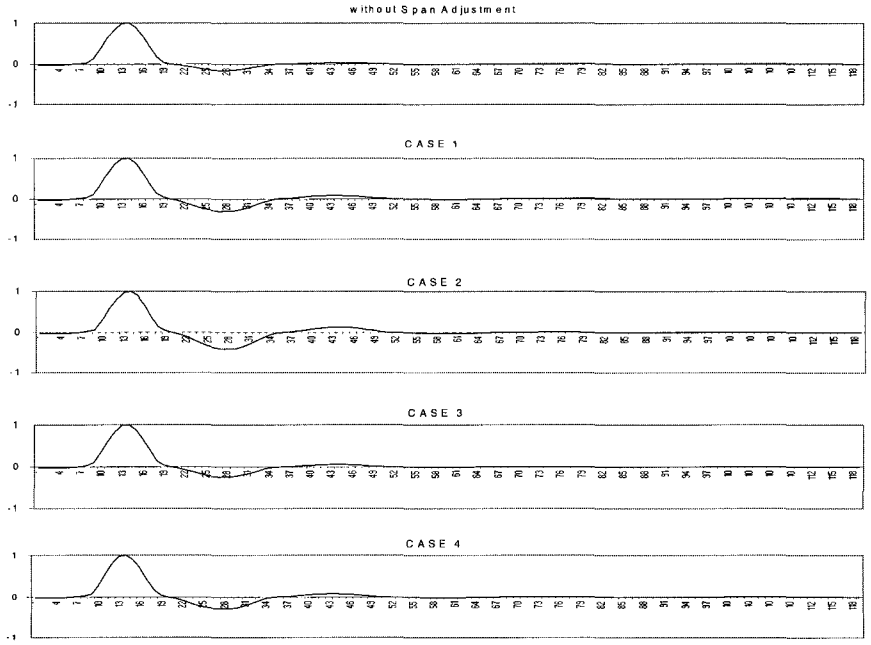

Fig. 7 1st Mode Shapes of Fuel Rod (Span Adjustment)

Table 6 Natural Frequencies of Fuel Rod-Support Condition, unit : Hz (Span Adjustment : +0.7 in., -0.3 in.)

Mode	Full Support Condition	Pinned Support Condition
1	36.80	25.72
2	45.07	32.07
3	49.94	37.79
4	50.44	40.31
5	102.65	77.43
6	121.52	78.30
7	124.29	80.46
8	128.18	83.07
9	133.46	86.30
10	137.05	89.02

first mode for the span adjustments are shown in Fig. 7. The change in natural frequencies for each case of span adjustment depends on the amount of span adjustments. There are no significant differences in the natural frequencies for each case of span adjustment. The natural frequencies of the first mode for the span adjustment are about 3 to 4Hz higher than that of the without span adjustment case. The higher natural frequencies are mainly due to the reduced span length of bottom span. The natural frequencies of the other modes for the span adjustment case are almost same as the case without span adjustment. The fuel rod mode shapes with more span adjustment has higher excitation at second span of fuel rod and less excitation at first span of fuel rod from bottom. Based on the results, the fuel rod with more span adjustment has better performance from fuel rod stability and fretting wear standpoint.

The natural frequencies for the support conditions are tabulated in Table 6 and the mode shapes for the support conditions are shown in Fig. 8. The natural frequencies of full support condition are higher than that of the pinned support condition. The decrease in natural frequencies for the pinned support condition is mainly due to the lack of fuel rod support. The mode shapes of pinned support condition are different from that of the full support condition. There is one single peak at first span of the fuel rod for the first mode of full support condition. On the other hand, there are several peaks at the bottom of the fuel rod for the first mode of pinned support condition. There is one single peak excitation at top span of fuel rod for the third mode of full support condition. The similar mode shape is shown in fourth mode of

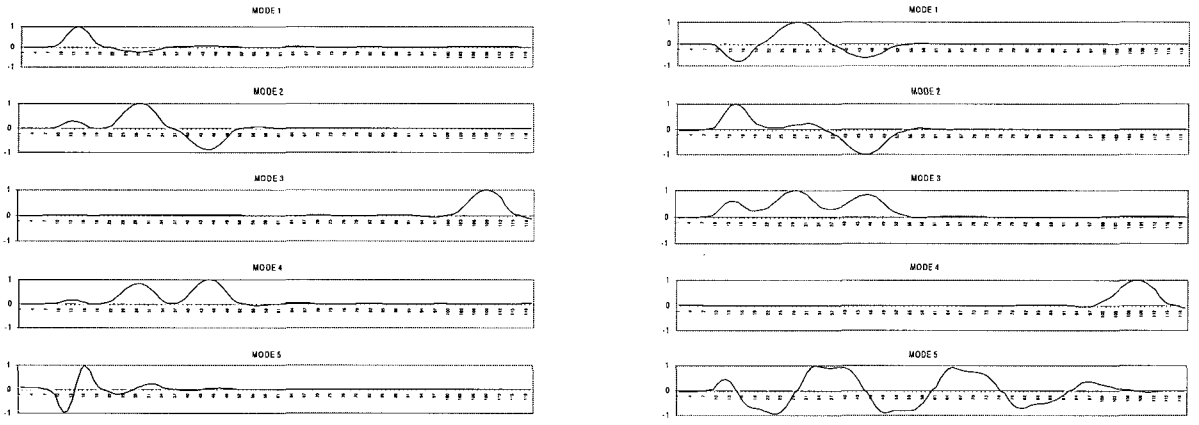

(a) Full Support Condition-with Span Adjustment (b) Pinned Support Condition-with Span adjustment

Fig. 8 Mode Shapes of Fuel Rod (Support Condition)

Table 7 Instability Ratio and Vibration Amplitude - Grid Height

(a) Instability Ratio

Mode	Grid Height=1.79 in.	Grid Height=2.25 in.	% Change
1	0.441	0.429	-2.72
2	0.648	0.563	-13.12
3	0.534	0.478	-10.49
4	0.577	0.546	-5.37
5	0.527	0.510	-3.23
6	0.503	0.500	-0.60
7	0.568	0.549	-3.35
8	0.173	0.169	-2.31
9	0.140	0.127	-9.29
10	0.128	0.113	-11.72

(b) Vibration Amplitude (unit : mils)

Mode	Grid Height=1.79 in.	Grid Height=2.25 in.	% Change
1	1.150	1.020	-11.30
2	0.452	0.311	-31.19
3	0.393	0.289	-26.46
4	0.309	0.259	-16.18
5	0.256	0.222	-13.28
6	0.222	0.207	-6.76
7	0.201	0.182	-9.45
8	0.056	0.053	-5.36
9	0.020	0.016	-20.00
10	0.017	0.014	-17.65

pinned support condition at top span of fuel rod. Based on the results, it is evaluated that the dynamic characteristics of fuel rod with pinned support condition are quite different from that of the fuel rod with full support condition. Also, it is evaluated that the pinned support condition need to be used to consider the end of life condition of fuel rod support in the core.

4.2 Instability Ratio and Vibration Amplitude

The instability ratio (V-Effective/V-Critical) and vibration amplitude for both the 1.79in. and 2.25 in. grid heights are tabulated in Table 7. The instability ratio and vibration amplitude of 2.25in. grid height is a little lower than that of 1.79in. grid height. Based on the results, the 2.25in. grid height has better performance considering fuel rod stability. However, it is judged that the fuel rod stability for both 2.25in. grid height and 1.79in. grid height would be similar because the differences are very small. The higher grid height has lower vibration amplitude compared to the lower grid height. This will result in improving the fretting wear performance for higher grid height.

The instability ratio and vibration amplitude for span adjustments are tabulated in Table 8. The instability ratio and vibration amplitude of the span adjustment cases are lower than that of the without span adjustment case. Based on the results, the fuel rod with span adjustment has better performance from the fuel rod stability and fretting wear standpoint. The improvement mainly depends on the amount of span adjustment of the first mid grid and bottom grid. There are some restrictions to move-up and move-down the spacer grids due to

Table 8 Instability Ratio and Vibration Amplitude - Span Adjustment

(a) Instability Ratio

Mode	Before Span Adjustment	After Span Adjustment (refer Table 3)			
		CASE 1	CASE 2	CASE 3	CASE 4
1	0.429	0.380	0.356	0.395	0.374
2	0.563	0.482	0.505	0.539	0.545
3	0.478	0.480	0.466	0.461	0.461
4	0.546	0.578	0.574	0.561	0.557
5	0.510	0.501	0.500	0.500	0.500
6	0.500	0.543	0.542	0.526	0.525
7	0.549	0.566	0.565	0.560	0.560
8	0.169	0.148	0.139	0.154	0.147
9	0.127	0.097	0.102	0.117	0.119
10	0.113	0.127	0.124	0.114	0.113

(b) Vibration Amplitude (unit : mils)

Mode	Before Span Adjustment	After Span Adjustment (refer Table 3)			
		CASE 1	CASE 2	CASE 3	CASE 4
1	1.020	0.774	0.684	0.847	0.759
2	0.311	0.290	0.293	0.306	0.307
3	0.289	0.289	0.284	0.280	0.280
4	0.259	0.284	0.281	0.268	0.268
5	0.222	0.241	0.241	0.234	0.233
6	0.207	0.217	0.217	0.212	0.211
7	0.182	0.192	0.192	0.188	0.188
8	0.053	0.041	0.036	0.044	0.040
9	0.016	0.017	0.016	0.015	0.015
10	0.014	0.016	0.016	0.015	0.015

the functional requirement of other components in the fuel assembly. The moving-up of the bottom grid is restricted by the grid-to-grid overlap requirement and the moving-down of the first mid grid is restricted by the grid to grid overlap requirement and the clearance requirement between first mid grid sleeve and guide thimble flow hole (Westinghouse, 1999). The first mid grid can be moved-down by 0.5in. and the bottom grid can be moved-up by 1.0in. due to the restrictions. Based on the results and restrictions, a new axial grid elevation for the advanced 16×16 fuel assembly development was proposed by evaluating the vibration characteristic and instability ratio for each span adjustment case. The proposed span adjustment considering these restrictions is moving-down the first mid grid by 0.5in. and moving-up the bottom grid by 1.0in.

The instability ratio and vibration amplitude for support conditions are tabulated in Table 9. The instability ratio and vibration amplitude of the pinned support condition are higher than that of the full support condition for both without and with span adjustment. However, the instability ratio of mode 3 of pinned support condition is lower than that of mode 3 of full support condition and the instability ratio of mode 4 of pinned support condition is much higher than that of mode 4 of full support condition comparing to instability ratio of other modes. It is evaluated that the higher instability ratio for mode 3 of full support condition and mode 4 of pinned support condition are due to the single peak of mode shape for mode 3 of full support condition and mode

Table 9 Instability Ratio and Vibration Amplitude - Support Condition

(a) Instability Ratio

Mode	without Span Adjustment		with Span Adjustment (+0.7 in., -0.3 in.)	
	Full Support	Pinned Support	Full Support	Pinned Support
1	0.375	0.384	0.339	0.321
2	0.110	0.290	0.120	0.302
3	0.612	0.178	0.619	0.198
4	0.098	0.739	0.100	0.747
5	0.149	0.188	0.135	0.172
6	0.137	0.212	0.137	0.201
7	0.122	0.189	0.111	0.212
8	0.115	0.196	0.124	0.187
9	0.133	0.199	0.134	0.202
10	0.102	0.155	0.098	0.152
11	0.130	0.185	0.139	0.185

(b) Vibration Amplitude (unit : mils)

Mode	without Span Adjustment		with Span Adjustment (+0.7 in., 0.3 in.)	
	Full Support	Pinned Support	Full Support	Pinned Support
1	1.009	1.653	0.812	1.567
2	0.316	0.916	0.334	0.824
3	0.377	0.508	0.387	0.489
4	0.230	0.645	0.254	0.660
5	0.052	0.081	0.042	0.044
6	0.021	0.051	0.021	0.050
7	0.016	0.045	0.016	0.045
8	0.016	0.046	0.017	0.041
9	0.018	0.043	0.018	0.044
10	0.014	0.034	0.012	0.032
11	0.014	0.037	0.015	0.037

4 of pinned support condition. It is also evaluated that the pinned support condition needs to be considered for the fuel rod stability analysis because the pinned supported condition is more realistic and conservative condition than the full support condition.

5. Conclusions

The fuel rod vibration and stability analyses were performed to investigate the effect of the grid height, support condition, and span adjustment on fuel rod vibration characteristics for the advanced 16x16 fuel assembly design.

(1) The higher grid height has lower instability ratio, lower vibration amplitude, and better fretting wear performance compare to the lower grid height. The natural frequencies of 2.25in. grid height are higher than that of the 1.79in. grid height and the instability ratio (V-Effective/V-Critical) and vibration amplitude of 2.25in. grid height is a little lower than that of 1.79in. grid height.

(2) The change in natural frequencies for each case of span adjustment depends on the amount of span adjustments. The natural frequencies of the first mode for the span adjustment are about 3 to 4Hz higher than that of the case without span adjustment. The fuel rod with span adjustment has better performance of the fuel rod stability and

fretting wear. The improvement depends on the amount of span adjustment of the first mid grid and bottom inconel grid. The proposed span adjustment considering some restrictions is moving-down the first mid grid by 0.5in. and moving-up the bottom inconel grid by 1.0in.

(3) The natural frequencies of full support condition are higher than that of the pinned support condition. The mode shapes of pinned support condition are different from those of full support condition. The instability ratio and vibration amplitude of the pinned support condition are higher than those of the full support condition for both without and with span adjustment. It is evaluated that the higher instability ratio for mode 3 of full support condition and mode 4 of pinned support condition are mainly due to the peak of mode shape for mode 3 of full support condition and mode 4 of pinned support condition. It is also evaluated that the pinned support condition needs to be considered for the fuel rod stability analysis because the pinned supported condition is more realistic and conservative condition than the full support condition.

Acknowledgement

This study has been carried out under the national nuclear mid & long term R&D program of the Ministry of Science and Technology (MOST).

References

ASME(1995) Section III, Division 1, Appendix N Article N-1000 Dynamic Analysis Methods.

Au-Yang, M. K.(2001) Flow-Induced Vibration of Power and Process Plant Components, *Professional Engineering Publishing Limited*, pp.155~196.

Kim, M. Y., Yun, H. T., Kwak, T. Y.(2002) Derivation of Exact Dynamic Stiffness Matrix of a Beam Column Element on Elastic Foundation, *Journal of Computational Structural Engineering*, 15(3), pp.463~469.

Lee, S. H., Park, T. H., Baek, J. W., Han, B. K.(2001) Free Vibration Analysis of Multi-Delaminated Beams, *Journal of Computational Structural Engineering*, 14(4), pp.469~479.

Paidoussis, M. P.(1973) Dynamics of Cylindrical Structure subjected to Axial Flow, *Journal of Sound and Vibration*, 29, pp.365~385.

Paidoussis, M. P., Mateescu, D., Woo, G. S. (1990) Dynamics and Stability of a Flexible Cylinder in a Narrow Coaxial Cylinder Duct subjected to Annular Flow, *Journal of Applied Mechanics*, 57, pp.232~240.

Park, N. G., Jeon, S. Y., Lee, S. H., Jeon, K. L., Lee, J. R., Kim, K. T., Dye, M. E.(2004) Dynamic Analysis of a Beam with Discretely Spaced Elastic Supports, *International Modal Analysis Conference XXII.*

Westinghouse(1989) WECAN User's Manual, Westinghouse Proprietary.

Westinghouse(1989) VIBAMP User's Manual, Westinghouse Proprietary.

Westinghouse(1999) Mechanical Design Manual, Westinghouse Proprietary.

Westinghouse(2000) THINC IV User's Manual, Westinghouse Proprietary.

Woo, G. S., Yoon, Y. B.(1994) Dynamic Stability of a Flexible Cylinder Subjected to Inviscid Flow in a Coaxial Cylinder Duct Based on Spectral Method, *Journal of the Korean Nuclear Society*, 26(2), pp.212~224.